NASA Technical Memorandum 81211 AVRADCOM Technical Report 80-A-14

A Conservative Implicit Finite Difference Algorithm for the Unsteady Transonic Full Potential Equation

Joseph L. Steger and Francis X. Caradonna

October 1980

NASA National Aeronautics and Space Administration

United States Army Aviation Research and Development Command

NASA Technical Memorandum 81211

AVRADCOM Technical Report 80-A-14

A Conservative Implicit Finite Difference Algorithm for the Unsteady Transonic Full Potential Equation

Joseph L. Steger, Flow Simulations, Inc., Sunnyvale, CA 94086
and
Francis X. Caradonna, Aeromechanics Laboratory, U.S. Army Research and Technology Laboratories, AVRADCOM, Ames Research Center, Moffet Field California 94035

NASA
National Aeronautics and Space Administration
Ames Research Center
Moffett Field, California 94035

United States Army
Aviation Research and Development Command
St. Louis, Missouri 63166

ABSTRACT

An implicit finite difference procedure is developed to solve the unsteady full potential equation in conservation-law-form. Computational efficiency is maintained by use of approximate factorization techniques. The numerical algorithm is first order in time and second order in space. A circulation model and difference equations are developed for lifting airfoils in unsteady flow, however, thin airfoil body-boundary conditions have been used with stretching functions to simplify the development of the numerical algorithm.

1. INTRODUCTION

Current numerical algorithms to compute unsteady transonic inviscid flow about complex configurations are frequently either inadequate or too costly to use for routine analysis of a large class of two and three dimensional flowfields. In particular, numerical algorithms[1,2,3] for unsteady transonic small disturbance theory neglect terms that can be important, for example, in helicopter rotor flowfield simulation. Numerical algorithms based on the Euler equations are suitable for any inviscid flowfield simulation, but current numerical algorithms for the Euler equations have large computer time and computer storage requirements. The successful development of an unsteady conservation-law-form full potential finite difference algorithm therefore offers a practical design tool. Unsteady potential theory can satisfactorily replace the Euler equation solutions if the shock waves are sufficiently weak and if the equations employ an equivalent circulation model. Yet, the full potential equation has similar computer requirements in time and storage to the simplified small disturbance theory.

The purpose of this paper is to present an approximate-factorization, implicit finite difference algorithm for the unsteady full potential equations in conservation-law-form. Conservation-law-form is maintained in order to "capture" shocks with correct strength and location. During the course of this research, two other unsteady procedures have been developed for the full potential equations in conservative form. One procedure, due to Chipman and Jameson[4] solves a system of three equations for three unknowns. The other, due to Goorjian,[5] is a scheme which is quite similar to the one developed independently here. In this report the governing equations are first reviewed in Section 2. Differencing of the governing equations in conservation-law-form and their numerical solution are discussed in Sections 3 and 4. Finally results and concluding remarks follow. Throughout small disturbance boundary conditions are used to avoid unduly complicating the development of the numerical method for the full potential equations.

2. GOVERNING EQUATIONS

Stretching Transformations

As governing equations for two-dimensional unsteady full potential flow we use the conservation of mass equation

$$\frac{\partial \rho}{\partial t} + \frac{\partial \rho \phi_x}{\partial x} + \frac{\partial \rho \phi_y}{\partial y} = 0 \tag{1}$$

where density, ρ, is determined from the unsteady Bernoulli relation

$$\rho = \{1 + \frac{\gamma - 1}{2}(M_\infty^2 - 2\phi_t - \phi_x^2 - \phi_y^2)\}^{\frac{1}{\gamma-1}} = a^{\frac{2}{(\gamma-1)}} \tag{2}$$

Here $\phi_x = u$, $\phi_y = v$ satisfy the condition of irrotationality

$$\frac{\partial u}{\partial y} - \frac{\partial v}{\partial x} = 0 \tag{3}$$

and in deriving Eq. (2) the far field flow is assumed to be steady. Throughout the equations have been referenced to freestream quantities,

$$\tilde{\rho} = \rho/\rho_\infty \ , \ \tilde{u} = u/a_\infty \ , \ \tilde{x} = x/\ell$$

and the tilda has been suppressed. Here a is the sound speed while ℓ is a reference length such as airfoil chord, c.

Boundary conditions are best satisfied by mappings which can also be used to cluster grid points so as to enhance numerical solution accuracy. As shown by Viviand[6] conservation-law-form of Eq. (1) can be maintained under the general transformation

$$\begin{aligned} \xi &= \xi(x, y, t) \\ \eta &= \eta(x, y, t) \\ \tau &= t \end{aligned} \tag{4}$$

giving

$$\frac{\partial}{\partial \tau}(\rho/J) + \frac{\partial}{\partial \xi}(\rho U/J) + \frac{\partial}{\partial \eta}(\rho V/J) = 0 \tag{5}$$

where J is the Jacobian $\xi_x \eta_y - \xi_y \eta_x$ and

$$\begin{aligned} U &= \xi_t + \xi_x \phi_x + \xi_y \phi_y = \xi_x(\phi_x - \dot{x}) + \xi_y(\phi_y - \dot{y}) \\ V &= \eta_t + \eta_x \phi_x + \eta_y \phi_y = \eta_x(\phi_x - \dot{x}) + \eta_y(\phi_y - \dot{y}) \end{aligned} \tag{6}$$

The terms ϕ_x and ϕ_y are expanded by chain rule

$$\begin{aligned} \phi_x &= \xi_x \phi_\xi + \eta_x \phi_\eta \\ \phi_y &= \xi_y \phi_\xi + \eta_y \phi_\eta \end{aligned} \tag{7}$$

and U and V can also be written

$$U = \xi_t + \nabla\xi \cdot (\phi_\xi \nabla\xi + \phi_\eta \nabla\eta) = \nabla\xi \cdot (\phi_\xi \nabla\xi + \phi_\eta \nabla\eta - \vec{r}_t) \tag{8a}$$

$$V = \eta_t + \nabla\eta \cdot (\phi_\xi \nabla\xi + \phi_\eta \nabla\eta) = \nabla\eta \cdot (\phi_\xi \nabla\xi + \phi_\eta \nabla\eta - \vec{r}_t) \tag{8b}$$

where $\vec{r} = (x, y)^t$. Subject to the same transformation the Bernoulli equation is written

$$\rho = \{1 + \frac{\gamma - 1}{2} [M_\infty^2 - 2(\phi_\tau + \xi_t \phi_\xi + \eta_t \phi_\eta) - (\xi_x^2 + \xi_y^2)\phi_\xi^2 - 2(\xi_x \eta_x + \xi_y \eta_y)\phi_\xi \phi_\eta - (\eta_x^2 + \eta_y^2)\phi_\eta^2]\}^{\frac{1}{\gamma-1}} \tag{9}$$

For the present purpose of demonstrating an unsteady full potential algorithm in conservation-law-form the transformation is restricted to the form

$$\begin{aligned} \xi &= \xi(x) \\ \eta &= \eta(y) \end{aligned} \tag{10}$$

and the thin-airfoil body-boundary approximation is utilized. Because of the transformation Eq. (10), the governing equations then simplify to

$$\frac{\partial(\rho/J)}{\partial\tau} + \frac{\partial}{\partial\xi}((\rho/J)\xi_x^2 \phi_\xi) + \frac{\partial}{\partial\eta}((\rho/J)\eta_y^2 \phi_\eta) = 0 \tag{11a}$$

$$\rho = \{1 + \frac{\gamma - 1}{2}(M_\infty^2 - 2\phi_\tau - \xi_x^2 \phi_\xi^2 - \eta_y^2 \phi_\eta^2)\}^{\frac{1}{\gamma-1}} \tag{11b}$$

Boundary Conditions

As boundary conditions, tangency (i.e. V = 0) is imposed on the body surface and the flow at infinity is required to be uniform and steady. The thin-airfoil body-boundary approximation is utilized

since our sole interest here is that of developing an efficient unsteady algorithm. The complete mapping of boundary conditions unduly complicates this task. Surface tangency $(\phi_x - \dot{x})\eta_x + (\phi_y - \dot{y})\eta_y = 0$ is replaced by

$$\phi_y = u_\infty \left.\frac{dy}{dx}\right|_{\text{body slope}} + \dot{y} \tag{12}$$

which is imposed on the grid lines adjacent to the airfoil -- see Fig. 1.

At distances far from the body $u = u_\infty$ and with our use of a_∞ as a reference velocity

$$\phi_\infty = M_\infty x \tag{13}$$

where M_∞ is the freestream Mach number. Here we chose to cant the airfoil to obtain angle of attack rather than have the flow vector be specified at an angle as is often done.

For lifting cases we must allow for a jump of potential across a cut. As we intend to partially model an unsteady shear layer leaving the airfoil, this cut is taken off from the trailing edge, see Fig. 1. On the back boundary then, Eq. (13) does not apply and so on the back boundary freestream pressure (or density in isentropic flow) is imposed. From Eq. (11b) this implies that

$$2\phi_\tau + \xi_x^2\phi_\xi^2 + \eta_y^2\phi_\eta^2 = M_\infty^2 \tag{14}$$

along the back face cd of Fig. 1a. Neglecting small perturbations, this simplifies to

$$\phi_\tau + \xi_x M_\infty \phi_\xi = M_\infty^2 \tag{15}$$

Eq. (13) is imposed along all other far field boundaries, Fig. 1a.

In unsteady flow, vorticity is continuously shed from the airfoil. In a potential flow formulation this phenomenon can be modeled with a cut aligned with the shear layer. Here we further idealize this cut by keeping it in the mean chord line plane as sketched in Fig. 1b.

The jump in potential along the cut, $\Delta\phi = \Gamma$, will vary with time. By imposing the usual shear layer assumptions an equation for $\Gamma(x, t)$ along the cut can be derived. Across an inviscid shear layer normal velocity and pressure (p) are continuous, while tangential velocity and density can be discontinuous. Here, however, the incoming flow is uniform isentropic (i.e. homentropic) and the shocks are weak. Thus, we have previously assumed that $p = \rho^{\gamma}$ throughout, and density is also taken to be continuous across the cut.

Define $\Gamma = [\![\phi]\!] = \phi_u - \phi_\ell$ across the cut as illustrated in Fig. 1b. From the condition that the velocity normal to the shear layer is continuous, $[\![\phi_y]\!] = 0$

$$\partial_y \phi_\ell = \partial_y \phi_u = \partial_y(\phi_\ell + \Gamma) \tag{16}$$

The Bernoulli relation together with the continuity of density and normal velocity requires that

$$(2\phi_t + \phi_x^2 + \phi_y^2)_\ell = (2\phi_t + \phi_x^2 + \phi_y^2)_u$$

or

$$(2\phi_t + \phi_x^2)_\ell = 2\partial_t(\phi_\ell + \Gamma) + [\partial_x(\phi_\ell + \Gamma)]^2 + [\partial_y(\phi_\ell + \Gamma)]^2$$

so that

$$2\Gamma_t + 2\phi_x\big|_\ell \Gamma_x + \Gamma_x^2 = 0 \tag{17}$$

Consistent with thin airfoil body boundary conditions, Eq. (17) is approximated by

$$\Gamma_t + M_\infty \Gamma_x = 0 \tag{18}$$

Eq. (18) gives an equation to determine $\Gamma(x, t)$ along the cut.

Although ϕ_y is continuous across the cut and $\Gamma_y = 0$, in unsteady flow and ϕ_{yy} is discontinuous. This follows immediately from

$$[\![\, \partial_t \rho + \partial_x(\rho\phi_x) + \partial_y(\rho\phi_y) \,]\!] = 0 \tag{19}$$

which on employing density continuity becomes

$$[\![\, \partial_x(\rho\phi_x) + \rho\partial_y \phi_y \,]\!] = 0 \tag{20}$$

or alternately

$$\rho[\![\, \phi_{yy} \,]\!] = - \partial_x(\rho\Gamma_x) \tag{21}$$

This last equation will be needed to develop accurate difference expressions for Eq. (11a) when it is differenced to just either side of the cut (see Section 4). For steady flow $\Gamma_t = 0$ and from Eq. (17) or (18) it follows that $\Gamma_x = 0$. Thus, in steady flow ϕ_{yy} is continuous across the cut.

3. CONSERVATIVE DIFFERENCING AND LOCAL LINEARIZATIONS

Time Derivative Term

Stable conservative difference operators have been successfully developed for the steady state part of Eqs. (1) or (11a) (see Refs. 7-10) so the main task initially undertaken in this research effort has been to develop stable conservative difference operators for the unsteady terms as well. Development of nonconservative time differencing schemes

has always appeared to be straightforward. Because $\rho = \rho(\phi)$, Eq. (1) can be rewritten as

$$\frac{\partial \rho}{\partial \phi}\frac{\partial \phi}{\partial t} + \rho\left(\frac{\partial^2 \phi}{\partial x^2} + \frac{\partial^2 \phi}{\partial y^2}\right) + \phi_x \frac{\partial \rho}{\partial \phi}\frac{\partial \phi}{\partial x} + \phi_y \frac{\partial \rho}{\partial \phi}\frac{\partial \phi}{\partial y} = 0 \tag{22}$$

where

$$\frac{\partial \rho}{\partial \phi} = -\rho^{2-\gamma}\left(\frac{\partial}{\partial t} + \phi_x \frac{\partial}{\partial x} + \phi_y \frac{\partial}{\partial y}\right) \tag{23}$$

is a differential operator that does not commute. Performing the indicated operations, Eq. (22) is found to be a second degree wave equation in nonconservative form

$$\phi_{tt} + 2\phi_x\phi_{xt} + 2\phi_y\phi_{yt} = (\rho^{\gamma-1} - \phi_x^2)\phi_{xx} - 2\phi_x\phi_y\phi_{xy} + (\rho^{\gamma-1} - \phi_y^2)\phi_{yy} \tag{24}$$

here using $\rho^{\gamma-1} = a^2$ (in the chosen nondimensional variables) gives the familiar textbook form of the potential equation (see, e.g. Ref. 11). Various finite difference schemes have been advanced for simpler but similar forms of this equation (1-3) and we assume they can be made to work for Eq. (24).

The problem arises, though, that Eq. (24) cannot be brought back into conservation-law-form with ϕ retained as the dependent variable. If, however, one is willing to introduce into the differential equations the same expansions used in deriving the difference formula, conservative form can again be maintained. By Taylor expansion

$$\rho = \rho_o + \frac{\partial \rho}{\partial \phi}\Big|_o(\phi - \phi_o) + O(\rho - \rho_o)^2 \tag{25}$$

where o represents a neighboring known state or solution. Substitution of Eq. (25) into Eq. (1) gives

$$\frac{\partial}{\partial t}\left\{\rho_o^{2-\gamma}\left(\frac{\partial}{\partial t} + \phi_x|_o \frac{\partial}{\partial x} + \phi_y|_o \frac{\partial}{\partial y}\right)\phi\right\} = \frac{\partial}{\partial x}(\rho\phi_x) + \frac{\partial}{\partial y}(\rho\phi_y)$$
$$+ \frac{\partial}{\partial t}\left(\rho_o - \frac{\partial\rho}{\partial\phi}|_o \phi_o\right) + O(\phi - \phi_o)^2 \qquad (26)$$

Assuming that all of the density terms are formed with exactly the same difference operators, we assume that the local linearization term $\partial_t\left(\rho_o - \frac{\partial\rho}{\partial\phi}|_o \phi_o\right)$ has only a higher order contribution to numerical stability. Moreover, if $\phi - \phi_o$ is small, for example $\phi^{n+1} - \phi^n$ or $\phi_j - \phi_{j-1}$ where $t = n\Delta t$ and $x = j\Delta x$, the error due to expanding ρ is second order accurate and is no greater than that usually made in time differencing.

Consequently, Eq. (26) is a conservation-law-form of Eq. (1) which is assumed to have linear stability properties equivalent to the equation

$$\frac{\partial}{\partial t}(\alpha_1\phi_t + \alpha_2\phi_x + \alpha_3\phi_y) = \partial_x(\rho\phi_x) + \partial_y(\rho\phi_y) + f_o \qquad (27)$$

As with the nonconservative form, Eq. (24), one can devise stable difference schemes for Eq. (27) when α_1, α_2, α_3, and ρ are considered as constants. With care, these schemes can be expected to apply for the nonlinear equations as well, although, as discussed immediately below, assuming ρ to be a constant fails for transonic flow. A correct treatment of the right-hand side of Eq. (27), however, is known from Refs. (7-10).

Space Derivatives

Just as the local linearization approach guides the proper treatment of the time derivative term, it can be used to analyze the space differencing schemes developed for the spatial terms of Eq. (1) by Jameson,[7] Holst and Ballhaus,[8] and Hafez, South, Murman[10] for transonic flow regions. Before proceeding with this analysis, however, some preliminary background information is in order.

Consider first the simple steady state model problem

$$(1 - M_\infty^2)\phi_{xx} + \phi_{yy} = 0 \tag{28}$$

and let ∇_x, Δ_x, ∇_y and Δ_y be defined in the conventional way, e.g. $\nabla_x\phi = (\phi_j - \phi_{j-1})/\Delta x$ and $\Delta_y\phi = (\phi_{k+1} - \phi_k)/\Delta y$. It is well known that the following difference schemes

$$(1 - M_\infty^2)\nabla_x\Delta_x\phi + \nabla_y\Delta_y\phi = 0 \qquad M_\infty < 1 \tag{29a}$$

$$(1 - M_\infty^2)\nabla_x\nabla_x\phi + \nabla_y\Delta_y\phi = 0 \qquad M_\infty > 1 \tag{29b}$$

are respectively suitable for the model elliptic ($M_\infty < 1$) and the model hyperbolic ($M_\infty > 1$) problems. The differencing (29b) is divergent if $M_\infty < 1$ while that of (29a) is convergent for $M_\infty > 1$ only if $|\Delta x/((1 - M_\infty^2)\Delta y)| \leq 1$, an impractical constraint for $M_\infty \to 1$. Murman and Cole,[12] aware of these simple constraints, introduced their type dependent different operators for the transonic small disturbance equation. In this approach the streamwise spatial difference operator is switched from central to backward as the local Mach number is less or greater than 1.

Various refinements to the Murman-Cole differencing have been introduced, but apparently overlooked is the fact that Eq. (28) can also be differenced as

$$\nabla_x \Delta_x \phi - M_\infty^2 \nabla_x \nabla_x \phi + \nabla_y \Delta_y \phi = 0 \qquad M_\infty \gtrless 1 \tag{30}$$

without any need to switch difference operators. An extra boundary condition is needed in the x-direction (which is also true of many higher order difference schemes) and one must pay attention to the physics because replacing $M_\infty^2 \nabla_x \nabla_x \phi$ by $M_\infty^2 \Delta_x \Delta_x \phi$ is also convergent for any M_∞. The differencing scheme given by Eq. (30) is also less accurate than Eq. (29a), but, subject to the usual approximations such as use of periodic boundary conditions, the authors can demonstrate the convergence of Eq. (30).

Although apparently not recognized as such, the difference schemes of Refs. (7-10), which are used when the local Mach number is > 1, actually mimic the differencing scheme represented by Eq. (30). The same differencing is not used in subsonic regions because the pure central differencing scheme is more accurate. The local linearization process will now be used to clarify these remarks.

Consider the spatial derivative term $\partial_x \rho \partial_x \phi$. Use of the local linearization, Eq. (23), with this term gives

$$\begin{aligned}
\partial_x \rho \phi_x &= \partial_x \left[(\rho \phi_x)_o + \left(\phi_x \frac{\partial \rho}{\partial \phi} + \rho \frac{\partial}{\partial x} \right)\Big|_o (\phi - \phi_o) \right] \\
&= \partial_x \left[\rho_o \partial_x \phi - (\phi_x \rho^{2-\gamma})_o (\partial_t + \phi_x|_o \partial_x + \phi_y|_o \partial_y)(\phi - \phi_o) \right] \\
&= \partial_x \left[\rho_o \partial_x \phi - (\rho \phi_x^2 / a^2)_o \partial_x \phi \right] - \partial_x ((\rho \phi_x / a^2) \partial_t \phi) - \partial_x ((\rho \phi_x \phi_y / a^2) \partial_y \phi) \\
&\quad - \partial_x f_o
\end{aligned} \tag{31}$$

The ϕ_{xt} and ϕ_{xy} terms of Eq. (31) are not crucial to our discussion, and we can justify ignoring them by assuming steady small perturbation flow. The bracket term of Eq. (31) is clearly a type dependent term of the form

$$\partial_x \rho_o \partial_x \phi - \partial_x \rho_o (u_o/a_o)^2 \underset{\sim}{\partial_x} \phi \tag{32}$$

where the subtilda is used as a reminder that this operator is the operator used in the Bernoulli equation to form ρ. Using the differencing formula of Refs. (7-10), the term $\partial_x \rho \phi_x$ of Eq. (1) is always treated by central difference formula, although in supersonic flow regions ρ is evaluated shifted back to the previous point in x. That is, the term $\partial_x \rho \partial_x \phi$ is replaced by (see Ref. 8 or 9)

$$(\partial_x \rho \partial_x \phi)_j = \partial_x [(1 - \nu)\rho + \nu \tilde{\rho}] \partial_x \phi \qquad \begin{cases} \nu = 0, (u/a)^2 < 1 \\ \nu = 1, (u/a)^2 > 1 \end{cases} \tag{33}$$

where $\tilde{\rho}$ is a shifted backward (i.e. upwind) value of density. The precise difference operators are treated in Appendix A; but, the crucial point to be made here is that when density is shifted backwards, the operator $\underset{\sim}{\partial}$ of Eq. (32) also is shifted backwards (upwind) as this operator comes from the local linearization of the Bernoulli equation. Thus the differencing Eq. (33) is equivalent to the differencing

$$\delta_x [(1 - \nu)\rho + \nu \tilde{\rho}] \delta_x \phi = \underbrace{\delta_x \rho_o \delta_x \phi}_{\text{central}} - \underbrace{\delta_x \rho_o (u_o^2/a_o^2) \delta_x \phi}_{\substack{\text{central } \nu = 0 \\ \text{backwards } \nu = 1}} + \ldots \tag{34}$$

where δ_x are symbolic difference operators. A rigorous discussion of the actual difference operators is given in Appendix A.

If the local linearization argument given above is indeed valid, then the differencing represented by Eq. (34) with $\nu = 1$ should be stable in subsonic as well as supersonic region so that switching is unnecessary. This is indeed the case as reported in Ref. 8, and, with the use of second order differencing, the unswitched differencing scheme gives quite satisfactory results as we later demonstrate.

4. NUMERICAL ALGORITHM

An implicit approximately factored (AF) finite difference scheme is developed for Eq. (11) in conservation-law-form by using the local linearization discussed in the previous section. The advantages of an implicit AF algorithm have been discussed before, see, for example Refs. 1, 2, 8, and 13. The algorithm presented here is optionally first or second order accurate in space and time, but the second order in time option has not proved to be satisfactory.

An implicit finite difference scheme for Eq. (11a) is given by (here suppressing spatial indices for convenience)

$$(\hat{\rho}^{n+1} - \hat{\rho}^{n}) + h\bar{\delta}_{\xi}[(\xi_x^2\hat{\rho})^{n+1}\bar{\delta}_{\xi}\phi^{n+1}] + h\bar{\delta}_{\eta}[(\eta_y^2\hat{\rho})^{n+1}\bar{\delta}_{\eta}\phi^{n+1}]$$

$$= (\alpha/3)(\hat{\rho}^{n} - \hat{\rho}^{n-1}) \qquad (35)$$

where $\hat{\rho} \equiv (\rho/J)$, $h = \frac{(3 - \alpha)\Delta t}{3}$ and $\alpha = 0$ for first order time accuracy or $\alpha = 1$ for second order time accuracy. The operators $\bar{\delta}_{\xi}$ and $\bar{\delta}_{\eta}$ are defined at each j, k point ($x = j\Delta x$, $y = k\Delta y$) by

$$\bar{\delta}_\xi(\hat{\rho}\xi_x^2\bar{\delta}_\xi\phi) = (\xi_x^2/J)_{j+1/2}\left[(1 - \nu_{j+1})\frac{\rho_{j+1} + \rho_j}{2}\right.$$

$$\left. + \nu_{j+1}\frac{(1 + \theta)\rho_j + (1 - \theta)\rho_{j-1}}{2}\right](\phi_{j+1} - \phi_j)$$

$$- (\xi_x^2/J)_{j-1/2}\left[(1 - \nu_j)\frac{\rho_j + \rho_{j-1}}{2} + \nu_j\frac{(1 + \theta)\rho_{j-1} + (1 - \theta)\rho_{j-2}}{2}\right](\phi_j - \phi_{j-1}) \quad (36a)$$

$$\bar{\delta}_\eta(\hat{\rho}\eta_y^2\bar{\delta}_\eta\phi) = (\eta_y^2/J)_{k+1/2}\frac{\rho_{k+1} + \rho_k}{2}(\phi_{k+1} - \phi_k)$$

$$- (\eta_y^2/J)_{k-1/2}\frac{\rho_k + \rho_{k-1}}{2}(\phi_k - \phi_{k-1}) \quad (36b)$$

here $\Delta\xi = \Delta\eta = 1$ and only the varying indices are indicated. The parameter $\theta = 2$ for second order spatial accuracy in supersonic regions, and $\theta = 1$ for first order accuracy. The switching parameter ν is defined in a way similar to Refs. 7-10 and

$$\nu = [1 - (\rho/\rho^*)^2]c \qquad 1 \le c < 10 \quad (37)$$

$\nu \equiv 0$ if $\nu < 0$, i.e. subsonic

$\nu \equiv 1$ if $\nu > 1$, i.e. supersonic

The parameter ν can be set to one throughout, but accuracy will be impaired unless θ is also set to 2. The operators (36a) and (36b) assume that the flow will be supersonic only in the positive x-direction (see e.g. Ref. 9 for extensions). The density is found from the Bernoulli equation with ($\Delta\xi = \Delta\eta = 1$)

$$\phi_\xi|_j \doteq (\phi_{j+1} - \phi_{j-1})/2 = \delta_\xi \phi_j \tag{38a}$$

$$\phi_\eta|_k \doteq (\phi_{k+1} - \phi_{k-1})/2 = \delta_\eta \phi_k \tag{38b}$$

$$\phi_\tau|^{n+1} \doteq [(2 + \alpha)(\phi^{n+1} - \phi^n) - \alpha(\phi^n - \phi^{n-1})]/(2\Delta t) = \delta_\tau \phi^{n+1} \tag{38c}$$

The metrics ξ_x and η_y are obtained from

$$\xi_x = 2/(x_{j+1} - x_{j-1}) \tag{39a}$$

$$\eta_y = 2/(y_{k+1} - y_{k-1}) \tag{39b}$$

while the term $(\xi_x^2/J)_{j+1/2}$ of Eq. (36a) is formed either as

$$(\xi_x^2/J)_{j+1/2} = [(\xi_x^2/J)_{j+1} + (\xi_x^2/J)_j]/2 \tag{40a}$$

or

$$(\xi_x^2/J)_{j+1/2} = [(\xi_x/J)_{j+1} + (\xi_x/J)_j]/[2(x_{j+1} - x_j)] \tag{40b}$$

The terms $(\xi_x^2/J)_{j-1/2}$, $(\eta_y^2/J)_{k+1/2}$, and $(\eta_y^2/J)_{k-1/2}$ receive similar treatment. If Eq. (40a) is used, it is essential to add

$$\overline{\delta}_\xi(\rho_\infty \xi_x^2/J)\overline{\delta}_\xi \phi_\infty \tag{41}$$

to the right-hand side of Eq. (35) to subtract out a numerical truncation error due to incomplete metric cancellation (see also Refs. 14 and 15). The term, relation (41), should equal 0 where $\phi_\infty = M_\infty x$ but this is not obtained if Eq. (40a) is used and the error can be very appreciable on a highly stretched grid. A similar correction in the Bernoulli equation isn't needed due to the choice of difference operators and stretchings.

The local linearization of Section 3 are now introduced. Using Eq. (25) to both expand ρ^{n+1} about ρ^n and to expand ρ^n about ρ^{n-1}, the terms $\rho^{n+1} - \rho^n$ of Eq. (35) are approximated

$$\hat{\beta}^{n+1} - \hat{\beta}^{n} = \left(\rho^{n}/J^{n+1} - (\beta^{n}/J^{n+1})[\delta_{\tau} + (\xi_x^2)^{n+1}\,\phi_{\xi}^{n}\delta_{\xi} + (\eta_y^2)^{n+1}\,\phi_{\eta}^{n}\delta_{\eta}](\phi^{n+1} - \phi^{n})\right)$$

$$- \left(\rho^{n-1}/J^{n} - (\beta^{n-1}/J^{n})[\delta_{\tau} + (\xi_x^2)^{n}\phi_{\xi}^{n-1}\delta_{\xi} + (\eta_y^2)^{n}\phi_{\eta}^{n-1}\delta_{\eta}](\phi^{n} - \phi^{n-1})\right) \quad (42)$$

where $\frac{\partial\rho}{\partial\phi}$ of Eq. (25) is replaced by Eq. (23) and $\beta = \rho^{2-\gamma}$. Here also the coefficients ϕ_{ξ} and ϕ_{η} are evaluated as indicated by Eq. (38), while δ_{τ}, δ_{ξ}, and δ_{η} are the same operators defined by Eq. (38). Note both ρ^{n+1} and ρ^{n} are linearized not just ρ^{n+1}, otherwise, conservation-law-form and second order accuracy is lost. The operators δ_{τ}, δ_{ξ}, and δ_{η} were defined by Eq. (38) because their form is dictated by the selection of difference operators used in the Bernoulli equation for density. These operators work on any product of elements to their right.

The second derivative terms are rearranged into delta form and ρ^{n+1} is eliminated as follows:

$$\bar{\delta}_{\xi}(\xi_x^2\hat{\rho})^{n+1}\bar{\delta}_{\xi}\phi^{n+1} = \bar{\delta}_{\xi}(\xi_x^2\hat{\rho})^{n+1}\bar{\delta}_{\xi}(\phi^{n+1} - \phi^{n}) + \bar{\delta}_{\xi}(\xi_x^2\hat{\rho})^{n+1}\bar{\delta}_{\xi}\phi^{n}$$

$$\doteq \bar{\delta}_{\xi}(\xi_x^2/J)^{n+1}\rho^{n}\bar{\delta}_{\xi}(\phi^{n+1} - \phi^{n})$$

$$+ \bar{\delta}_{\xi}(\xi_x^2/J)^{n+1}[\rho^{n} + \alpha(\rho^{n} - \rho^{n-1})]\bar{\delta}_{\xi}\phi^{n} \quad (43)$$

The η-term is treated in a similar fashion, and for $\alpha = 1$ second order time accuracy is maintained.

Applying Eqs. (42) and (43) to Eq. (35) gives the locally linearized form of the implicitly differenced governing equation:

$$\Big((\beta^n/J^{n+1})[\delta_\tau + (\xi_x^2)^{n+1}\phi_\xi^n\delta_\xi + (\eta_y^2)^{n+1}\phi_\eta^n\delta_\eta] - h\overline{\delta}_\xi(\xi_x^2/J)^{n+1}\rho^n\overline{\delta}_\xi$$

$$- h\overline{\delta}_\eta(\eta_y^2/J)^{n+1}\rho^n\overline{\delta}_\eta\Big)(\phi^{n+1} - \phi^n)$$

$$= (\beta^{n-1}/J^n)[\delta_\tau + (\xi_x^2)^n\phi_\xi^{n-1}\delta_\xi + (\eta_y^2)^n\phi_\eta^{n-1}\delta_\eta](\phi^n - \phi^{n-1}) + (1 - (\alpha/3))(\beta^n - \beta^{n-1})$$

$$+ h\Big(\overline{\delta}_\xi(\xi_x^2/J)^{n+1}[\rho^n + \alpha(\rho^n - \rho^{n-1})]\overline{\delta}_\xi\phi^n + \overline{\delta}_\eta(\eta_y^2/J)^{n+1}(\rho^n + \alpha(\rho^n - \rho^{n-1})]\overline{\delta}_\eta\phi^n\Big) \quad (44)$$

where one must remember that the operators work on any product of terms to their right, e.g.

$$(\delta_\eta a\delta_\eta + \delta_\xi b\delta_\xi)(c + d) = \delta_\eta a\delta_\eta c + \delta_\eta a\delta_\eta d + \delta_\xi b\delta_\xi c + \delta_\xi b\delta_\xi d$$

The operator δ_τ that appears in Eq. (44) is given by Eq. (38c). As it operates on $\Delta\phi$, however, we chose to replace it by the operator

$$\delta_\tau\phi^{n+1} \doteq (\phi^{n+1} - \phi^n)/(\Delta t) \equiv (1/\Delta t)(I - E^{-1})\phi^{n+1} \quad (45)$$

which agrees with Eq. (38c) only if $\alpha = 0$. Eq. (45) is now substituted into Eq. (44), $\beta^n/(J^{n+1}\Delta t) = (\rho^{2-\gamma})^n/(J^{n+1}\Delta t)$ is divided through, and the left-hand side is approximately factored into ξ and η operators:

$$\{I + \Delta t(\eta_y^2)^{n+1}\phi_\eta^n\delta_\eta - \Delta t(J^{n+1}/\beta^n)h\overline{\delta}_\eta(\eta_y^2/J)^{n+1}\rho^n\overline{\delta}_\eta\}x$$

$$\{I + \Delta t(\xi_x^2)^{n+1}\phi_\xi^n\delta_\xi - \Delta t(J^{n+1}/\beta^n)h\overline{\delta}_\xi(\xi_x^2/J)^{n+1}\rho^n\overline{\delta}_\xi\}(\phi^{n+1} - \phi^n)$$

$$= [1 + (\beta^{n-1}/\beta^n)(J^{n+1}/J^n)](\phi^n - \phi^{n-1}) - (\beta^{n-1}/\beta^n)(J^{n+1}/J^n)(\phi^{n-1} - \phi^{n-2})$$

$$+ \Delta t(\beta^{n-1}/\beta^n)(J^{n+1}/J^n)[(\xi_x^2)^n\phi_\xi^{n-1}\delta_\xi + (\eta_y^2)^n\phi_\eta^{n-1}\delta_\eta](\phi^n - \phi^{n-1})$$

$$+ \Delta t(J^{n+1}/\beta^n)\{[1 - (\alpha/3)](\beta^n - \beta^{n-1}) + h\overline{\delta}_\xi(\xi_x^2/J)^{n+1}[\rho^n + \alpha(\rho^n - \rho^{n-1})]\overline{\delta}_\xi\phi^n$$

$$+ h\overline{\delta}_\eta(\eta_y^2/J)^{n+1}[\rho^n + \alpha(\rho^n - \rho^{n-1})]\overline{\delta}_\eta\phi^n\} \quad (46)$$

This equation has the form

$$L_\eta L_\xi(\phi^{n+1} - \phi^n) = R \tag{47}$$

and it is implemented as an algorithm as

$$L_\eta \Delta\phi^* = R \tag{48a}$$

$$L_\xi \Delta\phi^n = \Delta\phi^* \tag{48b}$$

$$\phi^{n+1} = \phi^n + \Delta\phi^n \tag{48c}$$

The algorithm Eq. (48) requires only a series of scalar tridiagonal inversions and it is therefore very efficiently implemented. Computer storage equivalent to four levels of ϕ have to be supplied with ρ computed from the Bernoulli equation as needed. Alternately three levels of ϕ and one level of ρ can be used, although in our test program two levels of ρ where stored for convenience in programming ` computer code that changed from day to day. All exponential functions were eliminated by using binomial expansions of the form:

$$\rho = 1 + \psi\varepsilon(1 + \frac{\psi-1}{2}\varepsilon(1 + \frac{\psi-2}{3}\varepsilon(1 + \frac{\psi-3}{4}\varepsilon))) \tag{49}$$

where

$$\varepsilon = (\gamma - 1)(M_\infty^2 - 2\phi_\tau - \xi_x^2\phi_\xi^2 - \eta_y^2\phi_\eta^2)/2$$

$$\psi = 1/(\gamma - 1)$$

and

$$\beta = \beta^*(1 + \psi\varepsilon(1 + \frac{\psi-1}{2}\varepsilon(1 + \ldots))) \tag{50}$$

where the constant $\beta^* = (\rho^*)^{2-\gamma}$ is evaluated using the nondimensional critical density, and

$$\varepsilon = (\rho/\rho^*) - 1$$

$$\psi = 2 - \gamma$$

The expansion for density gives at least four-place accuracy in the flow regime of interest. The expansion for β need not be so accurate as it is a linearization coefficient. On the CDC 7600 a run time of 90 seconds was reduced to 60 seconds because of the use of the expansions. In this example the solution was advanced 400 times steps on a 50 x 62 grid.

Implementation of Boundary Conditions

The thin-airfoil body-boundary tangency condition, Eq. (12), was directly built into the implicit algorithm. Indeed, it was in order to satisfy this boundary condition that η-tridiagonals are formed before the ξ-tridiagonals in Eq. (46) or (47). The difference equation (+/- indicate upper or lower surface)

$$\phi_k - \phi_{k\pm1} = (\mp M_\infty \left.\frac{dy}{dx}\right|_\pm + \frac{dy}{dt})/(\eta_y)_k \qquad (51)$$

is implemented into the numerical algorithm as follows: Eq. (48a) is first formed just as before ignoring the boundary. Then for points immediately above and below the airfoil chord -- which is centered in between, see Fig. 1 -- Eq. (51) is used to correctly overload the tridiagonal elements as sketched ir Fig. 2. Likewise, in forming the ξ-tridiagonals adjacent to the body-boundary, elements are first loaded as usual and then those elements corresponding to points just above or below the body are overloaded as sketched in Fig. 3. This approach insures that $\Delta\phi$ above and

below the airfoil are unaltered by the XI-inversions, yet come in implicitly for XI-derivatives just ahead and behind the airfoil leading edge and trailing edge.

Adjustments to the difference equations and numerical algorithm must also be made for points just above and below the cut indicated in Fig. 1. For these points, ϕ_η is altered as follows (see Appendix B)

$$\phi_\eta|_k = (\phi_{k+1} - \phi_{k-1} - \Gamma)/2 + [J/(16\rho\eta_y^2)]\overline{\delta}_\xi(\rho\xi_x^2/J)\overline{\delta}_\xi\Gamma \tag{52}$$

where this change effects the calculation of density as well as coefficients in Eq. (46). As indicated by Eq. (21), the difference formula for $\partial_\eta\hat{\rho}\eta_y^2\partial_\eta\phi$ must also be adjusted for points adjacent to the cut. For points above the cut (see the derivation in Appendix B)

$$\begin{aligned}\overline{\delta}_\eta\hat{\rho}\eta_y^2\overline{\delta}_\eta\phi = {} & (\eta_y^2/J)_{k+1/2}\frac{\rho_{k+1}+\rho_k}{2}(\phi_{k+1}-\phi_k) \\ & - (\eta_y^2/J)_{k-1/2}\frac{\rho_k+\rho_{k-1}}{2}(\phi_k - \phi_{k-1} - \Gamma) - 1/8\ \overline{\delta}_\xi(\rho\xi_x^2/J)\overline{\delta}_\xi\Gamma\end{aligned} \tag{53}$$

while for points below the cut

$$\begin{aligned}\overline{\delta}_\eta\hat{\rho}\eta_y^2\overline{\delta}_\eta\phi = {} & (\eta_y^2/J)_{k+1/2}\frac{\rho_{k+1}+\rho_k}{2}(\phi_{k+1}-\phi_k-\Gamma) \\ & - (\eta_y^2/J)_{k-1/2}\frac{\rho_k+\rho_{k-1}}{2}(\phi_k - \phi_{k-1}) + 1/8\ \overline{\delta}_\xi(\rho\xi_x^2/J)\overline{\delta}_\xi\Gamma\end{aligned} \tag{54}$$

For simplicity the term $1/8\ \overline{\delta}_\xi\hat{\rho}\xi_x^2\overline{\delta}_\xi\Gamma$ is lagged at time level n and it thus only enters into the right-hand side of Eq. (46).

At the end of each update of the field for ϕ, new values of Γ are obtained along the cut by solving Eq. (16). This equation is differenced as

$$\frac{\Gamma_j^{n+1}-\Gamma_j^n}{\Delta t} + \xi_x^2|_j\,(\Gamma_j^n - \Gamma_{j-1}^n + \phi_j^{n+1} - \phi_{j-1}^{n+1})(\Gamma_j^{n+1} - \Gamma_{j-1}^{n+1}) = \xi_x^2|_j(\Gamma_j^n - \Gamma_{j-1}^n)^2/2 \tag{55}$$

with initial data in x supplied from the known value of $\phi_u - \phi_\ell$ at the airfoil trailing edge just upstream of the cut.

5. RESULTS

Calculations to verify the accuracy of the numerical algorithm are shown in Figs. 4 to 7. The C_p distribution for steady-state flow about a 6 percent thick biconvex airfoil is shown in Fig. 4 for $M_\infty = 0.857$ and $\alpha = 1°$ angle of attack. The conservative full potential result obtained using the second order option, $\theta = 2$, is compared to experiment and a small disturbance nonconservative result. The conservatively captured shock is, of course, downstream of the nonconservative result. In this case the vertical far field boundaries are placed at 20 chord lengths away from the body, although equivalent results are obtained if these boundaries are as close as 12 chords.

As shown by the results of Fig. 5, essentially the same steady-state solution is obtained if the switching parameter ν is always set equal to 1 (i.e., no switching), provided the second order differencing $\theta = 2$ is used. Slight differences in the two solutions are observed at the leading edge singularity and at the shock wave. The unswitched scheme, $\nu = 1$, $\theta = 2$. gives a more pleasing shock wave result.

Unsteady solution accuracy is demonstrated by a comparison with a small disturbance low frequency result obtained by Ballhaus and Steger.[1] In this test case, the airfoil is a biconvex profile which varies in time from zero thickness to 10 percent thick, and then thins back to zero. A shock initially forms past mid-chord, and then moves back to the trailing edge as the airfoil thickens. As the airfoil then thins, the backward motion of the shock stops, and then the shock propagates upstream. Fig. 6 shows a trace of mid-chord pressure for such a case with a comparison to

the low frequency small disturbance result. The small discrepancy between the theories is about what one would expect for this case, and similar results are obtained with the full potential schemes of Goorjian.[5]

As a final test case the unsteady flow about an impulsively plunged flat plate was computed with $M_\infty = 0.8$ and a plunge velocity equivalent to $\alpha = 1°$. Linear theory is valid for this case and good agreement with linear theory is obtained by Chipman and Jameson[4] who solved the full potential, as well as by Beam and Warming[16] who solve the Euler equations. Good agreement with linear theory is also obtained with the present code as the load distributions plotted in Fig. 7 illustrate.

6. CONCLUDING REMARKS

An implicit finite difference procedure was developed to solve the unsteady full potential equation in conservation-law-form. Local linearizations were successfully used to derive a correct time differencing, avoid iteratives between time levels, and to correctly analyze the spatial differencing. An unsteady circulation model was developed and various test cases were done to verify the accuracy of the numerical algorithm.

REFERENCES

1. Ballhaus, W. F. and Steger, J. L., "Implicit Approximate Factorization Schemes for the Low-Frequency Transonic Equation," NASA TM X-73,082, 1975.

2. Ballhaus, W. F. and Goorjian, P. M., "Implicit Finite-Difference Computations of Unsteady Transonic Flows About Airfoils," AIAA Journal, Vol. 15, December 1977.

3. Caradonna, F. X. and Isom, M. P., "Numerical Calculation of Unsteady Transonic Potential Flow Over Helicopter Rotor Blades," AIAA Paper 75-168, January 1975.

4. Chipman, R. and Jameson, A., "Fully Conservative Numerical Solutions for Unsteady Irrotational Transonic Flow About Airfoils," AIAA Paper 79-1555, 1979.

5. Goorjian, P. M., "Computations of Unsteady Transonic Flow Governed by the Conservative Full Potential Equations Using an Alternating Direction Implicit Algorithm," NASA CR-152274, 1979.

6. Viviand, H., "Conservative Forms of Gas Dynamic Equations," La Recherche Aerospatiale, No. 1, January-February 1974, pp. 65-68.

7. Jameson, A., "Transonic Potential Flow Calculations Using Conservative Form," AIAA Second Computational Fluid Dynamics Conference Proceedings, June 1975, pp. 148-155.

8. Holst, T. L. and Ballhaus, W. F., "Fast Conservative Schemes for the Full Potential Equation Applied to Transonic Flows," NASA TM-78469, 1978. (Also AIAA Journal, Vol. 17, No. 2, February 1979, pp. 145-152).

9. Holst, T. L., "A Fast, Conservative Algorithm for Solving the Transonic Full-Potential Equation," AIAA Fourth Computational Fluid Dynamics Conference Proceedings, July 1979, pp. 109-121.

10. Hafez, M., South, J., and Murman, E., "Artificial Compressibility Methods for Numerical Solutions of Transonic Full Potential Equation," AIAA Journal, Vol. 17, August 1979, pp. 838-844.

11. Guderley, K. G., "The Theory of Transonic Flow," Addison-Wesley Publishing Company, Inc., Reading, Massachusetts, 1962.

12. Murman, E. M. and Cole, J. D., "Calculation of Plane Steady Transonic Flow," AIAA Journal, Vol. 9, 1971, pp. 114-121.

13. Warming, R. F. and Beam, R. M., "On the Construction and Application of Implicit Factored Schemes for Conservation Laws," SIAM-AMS Proceedings, Vol. 11, April 1977.

14. Steger, J. L., "Implicit Finite Difference Solution of Flow About Arbitrary Two-Dimensional Geometries," AIAA Journal, 16, 1978.

15. Pulliam, J. H. and Steger, J. L., "On Implicit Finite-Difference Simulations of Three Dimensional Flow," AIAA Paper 78-10, January 1978.

16. Beam, R. M. and Warming, R. F., "Numerical Calculations of Two-Dimensional, Unsteady Transonic Flows with Circulation," NASA TN D-7605, 1974.

APPENDIX A

Details are given in this appendix to show, to first approximation, the equivalence of Eq. (31) for the actual difference operators used in the Holst-Ballhaus delayed density scheme. Holst and Ballhaus have previously shown the equivalence of their scheme to the artificial viscosity method of Jameson[7] and of Hafez, South, and Murman.[12]

To make the steps clear, the analysis will be detailed here for the fully delayed case, $\nu = 1$ in Eq. (33), in one-dimensional steady flow. Then to first approximation it will be shown that

$$\frac{\rho_{j-1/2}(\phi_{j+1} - \phi_j) - \rho_{j-3/2}(\phi_j - \phi_{j-1})}{(\Delta x)^2} = \bar{\rho} \frac{(\phi_{j+1} - 2\phi_j + \phi_{j-1})}{\Delta x^2}$$

$$- \bar{\rho}^{2-\gamma} \bar{\phi}_x^2 \frac{(\phi_j - 2\phi_{j-1} + \phi_{j-2})}{\Delta x^2} \quad (A.1)$$

where ϕ_x in the Bernoulli equation is computed with the midpoint rule, e.g.

$$\phi_x = \delta_x \phi_j = \frac{\phi_{j+1/2} - \phi_{j-1/2}}{\Delta x} \quad (A.2)$$

To verify Eq. (A.1) the terms are expanded as follows:

$$\rho_{j-1/2} \frac{(\phi_{j+1} - \phi_j)}{\Delta x} \equiv \rho_{j-1/2} \delta_x \phi_{j+1/2}$$

$$= [\bar{\rho} + (\rho_{j-1/2} - \bar{\rho})] \delta_x (\bar{\phi} + \phi_{j+1/2} - \bar{\phi})$$

$$= \bar{\rho} \delta_x \bar{\phi} + \bar{\rho} \delta_x (\phi_{j+1/2} - \bar{\phi})$$

$$+ (\rho_{j-1/2} - \bar{\rho}) \delta_x \bar{\phi} + O(\Delta^2)$$

$$= \bar{\rho} \delta_x \phi_{j+1/2} + \bar{\phi}_x (\rho_{j-1/2} - \bar{\rho}) + O(\Delta^2) \quad (A.3)$$

where $\bar{\phi}$ and $\bar{\rho}$ are from a known nearby solution and $\bar{\phi}_x = \delta_x \bar{\phi}$.

From the steady one-dimensional Bernoulli equation

$$\rho = [1 + \frac{\gamma - 1}{2} (M_\infty^2 - \phi_x^2)]^{\frac{1}{\gamma-1}} \tag{A.4}$$

and via Taylor series

$$\rho = \bar{\rho} - \bar{\rho}^{2-\gamma}\bar{\phi}_x\partial_x(\phi - \bar{\phi}) + O(\Delta^2) \tag{A.5}$$

Using (A.5) to eliminate $\rho_{j-1/2} - \bar{\rho}$ from (A.3) gives

$$\rho_{j-1/2} \frac{(\phi_{j+1} - \phi_j)}{\Delta x} = \bar{\rho}\delta_x\phi_{j+1/2} - \bar{\rho}^{2-\gamma}\bar{\phi}_x^2\delta_x(\phi_{j-1/2} - \bar{\phi}) + O(\Delta^2) \tag{A.6}$$

where the midpoint rule Eq. (A 2) is again used to approximate derivatives. Likewise

$$\rho_{j-3/2} \frac{(\phi_j - \phi_{j-1})}{\Delta x} = \bar{\rho}\delta_x\phi_{j-1/2} - \bar{\rho}^{2-\gamma}\bar{\phi}_x^2\delta_x(\phi_{j-3/2} - \bar{\phi}) + O(\Delta^2) \tag{A.7}$$

Subtracting (6) from (7) and dividing by Δx gives Eq. (A.1) plus a term of $[O(\Delta^2) - O(\Delta^2)]/\Delta x = O(\Delta^2)$.

Other ways of shifting the density function give the first approximations:

(centered)

$$\frac{\rho_{j+1/2}(\phi_{j+1} - \phi_j) - \rho_{j-1/2}(\phi_j - \phi_{j-1})}{\Delta x^2} = (\bar{\rho} - \bar{\rho}^{2-\gamma}\phi_x^2)\frac{(\phi_{j+1} - 2\phi_j + \phi_{j-1})}{\Delta x^2} \tag{A.8}$$

(centered - upwind)

$$\frac{(2\rho_{j-1/2} - \rho_{j-3/2})(\phi_{j+1} - \phi_j) - (2\rho_{j-3/2} - \rho_{j-5/2})(\phi_j - \phi_{j-1})}{\Delta x^2}$$

$$= \bar{\rho}\frac{(\phi_{j+1} - 2\phi_j + \phi_{j-1})}{\Delta x^2} - \bar{\rho}^{2-\gamma}\bar{\phi}_x^2\frac{(2\phi_j - 5\phi_{j-1} - 4\phi_{j-2} + \phi_{j-3})}{(\Delta x)^2} \tag{A.9}$$

both of which are second order accurate approximations.

The difference schemes used in Section 4 do not use the mid-point rule to evaluate ϕ_x in the Bernoulli equation. Rather $\rho_{j-1/2}$ is approximated by $(\rho_j + \rho_{j-1})/2$ and ϕ_x is approximated with the three point relation, Eq. (38a). This gives the first approximation

$$\frac{\frac{(\rho_j + \rho_{j-1})}{2}(\phi_{j+1} - \phi_j) - \frac{(\rho_{j-1} + \rho_{j-2})}{2}(\phi_j - \phi_{j-1})}{\Delta x^2}$$

$$= \bar{\rho}\,\frac{(\phi_{j+1} - 2\phi_j + \phi_{j-1})}{\Delta x^2} - \bar{\rho}^{2-\gamma}\bar{\phi}_x^2\,\frac{(\phi_{j+1} - 2\phi_{j-1} + \phi_{j-3})}{(2\Delta x)^2} \qquad \text{(A.10)}$$

Unlike Eq. (A.1) a pure upwind formula is not used with the negative coefficient, $-\bar{\rho}^{2-\gamma}\bar{\phi}_x^2$. The resulting formula, however, is sufficiently biased to obtain the same effect. In fact, the combined differencing can be more upwind than (A.1) since the coefficient to the j+1 point is $\rho(1 - u^2/(4a^2))$ rather than $\bar{\rho}$.

APPENDIX B

The derivation of Eq. (53) is sketched below using the notation indicated in Fig. B.1. The derivative $\partial_y \rho \partial_y \phi$ is first approximated as

$$\partial_y \rho \partial_y \phi \Big|_k = \frac{(\rho_{k+1} + \rho_k)(\phi_{k+1} - \phi_k) - (\rho_k + \rho_{k-1})(\phi_y|_{k-1/2})\Delta y}{2(\Delta y)^2} + O(\Delta y) \qquad (B.1)$$

Now

$$\phi_k = \phi_u + \frac{\Delta y}{2} \phi_y|_u + 1/2 \left(\frac{\Delta y}{2}\right)^2 \phi_{yy}|_u$$

$$\phi_{k-1} = \phi_\ell - \frac{\Delta y}{2} \phi_y|_\ell + 1/2 \left(\frac{\Delta y}{2}\right)^2 \phi_{yy}|_\ell$$

or

$\phi_y|_{k-1/2} = \phi_y|_u = \phi_y|_\ell$ is found to be

$$\phi_y|_{k-1/2} = \left((\phi_k - \phi_{k-1}) - \Gamma - \frac{(\Delta y)^2}{8} (\phi_{yy}|_u - \phi_{yy}|_\ell)\right)/\Delta y$$

or

$$\Delta y \phi_y|_{k-1/2} = (\phi_k - \phi_{k-1} - \Gamma) - \frac{(\Delta y)^2}{8} [\![\phi_{yy}]\!] \qquad (B.2)$$

Approximating Eq. (21) as

$$\frac{\rho_k + \rho_{k-1}}{2} [\![\phi_{yy}]\!] = - \overline{\delta}_x \frac{\rho_k + \rho_{k-1}}{2} \overline{\delta}_x \Gamma \qquad (B.3)$$

and substituting Eq. (B.2) and Eq. (B.3) into Eq. (B.1) gives

$$\partial_y \rho \partial_y \phi \Big|_k = \frac{(\rho_{k+1} - \rho_k)(\phi_{k+1} - \phi_k) - (\rho_k + \rho_{k-1})(\phi_k - \phi_{k-1} - \Gamma)}{2(\Delta y)^2}$$

$$+ \frac{1}{8} \overline{\delta}_x \left(\frac{\rho_k + \rho_{k-1}}{2}\right) \overline{\delta}_x \Gamma \qquad (B.4)$$

Eq. (53) differs from (B.4) only in the addition of metrics.

The derivation of Eqs. (52) and (54) proceed in a similar way where in deriving Eq. (52) one starts with (for k above the cut)

$$\phi_\eta\big|_k = 1/2\left(\frac{\phi_{k+1} - \phi_k}{\Delta\eta} - \phi_\eta\big|_{k-1/2}\right) \ , \ \Delta\eta = 1 \qquad \text{(B.5)}$$

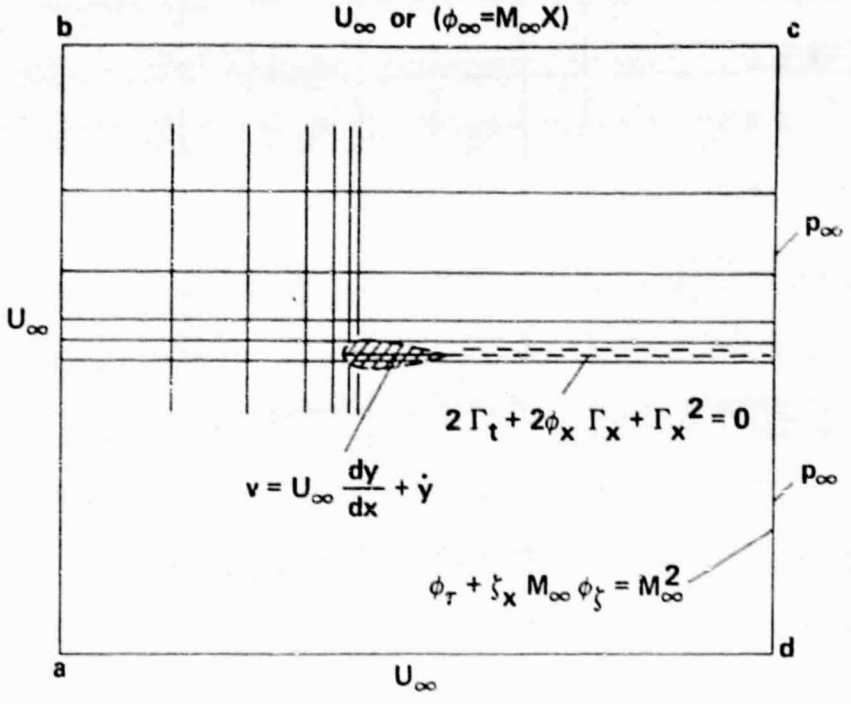

a)

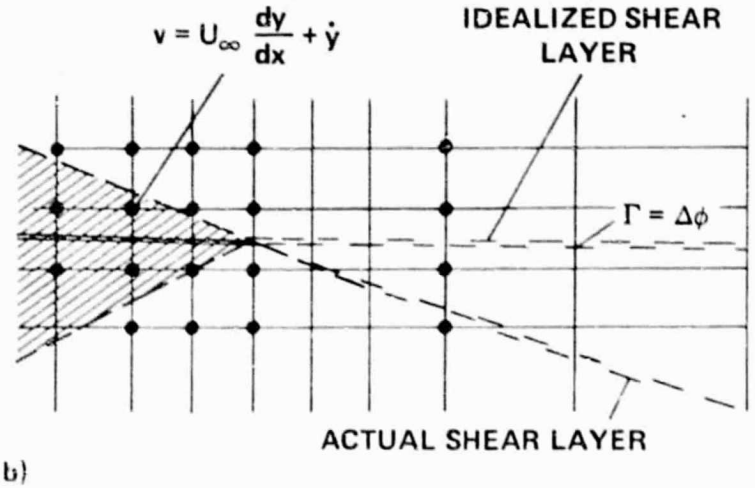

b)

Fig. 1. Schematic showing boundary conditions

$$\begin{bmatrix} B & C & & & & & \\ A & B & C & & & & \\ & \ddots & \ddots & \ddots & & & \\ & & A & B & C & & \\ & & & A & B & C & \\ & & & & A & B & C \\ & & & & & \ddots & \ddots \end{bmatrix} \Delta \begin{bmatrix} \phi_2 \\ \phi_3 \\ \\ \\ \phi_{M-1} \\ \phi_M \\ \phi_N \\ \phi_{N+1} \end{bmatrix} = \begin{bmatrix} R_2 - A\Delta\phi_1 \\ R_3 \\ \vdots \\ \\ R_{M-1} \\ R_M \\ R_N \\ R_{N+1} \\ \vdots \end{bmatrix}$$

(a) Tridiagonal $L_\eta \Delta\phi^* = R$ before tangency boundary condition

$$\begin{bmatrix} B & C & & & & & \\ A & B & C & & & & \\ & \ddots & \ddots & \ddots & & & \\ & & A & B & C & & \\ & & -I & I & & & \\ & & & I & -I & & \\ & & & A & B & C & \\ & & & & \ddots & \ddots & \ddots \end{bmatrix} \Delta \begin{bmatrix} \phi_2 \\ \phi_3 \\ \\ \\ \phi_{M-1} \\ \phi_M \\ \phi_N \\ \phi_{N+1} \\ \vdots \end{bmatrix} = \begin{bmatrix} R_2 - A\Delta\phi_1 \\ R_3 \\ \vdots \\ \\ R_{M-1} \\ -\Delta Y M_\infty Y\acute{e} - \phi_M - \phi_{M-1} \\ \Delta Y M_\infty Y\acute{u} - \phi_N + \phi_{N+1} \\ R_{N+1} \\ \vdots \end{bmatrix}$$

(b) Tridiagonal $L_\eta \Delta\phi^* = R$ with body tangency

Note: Indices on A, B, C, and * on $\Delta\phi^*$ are deleted; here $M = k_{lower}$, $N = k_{upper}$

Fig. 2. Adjustment of η-tridiagonal to implicitly include the thin-airfoil body-boundary condition

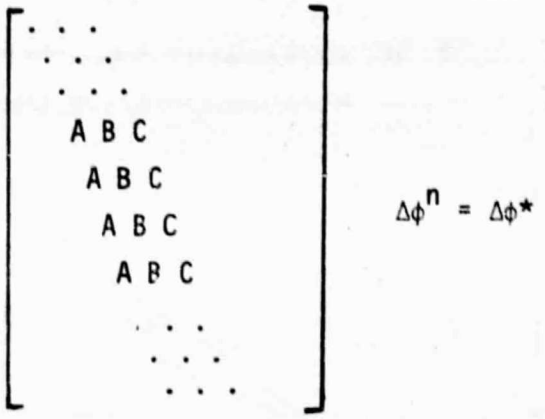

(a) Tridiagonal $L_\xi \Delta\phi^n = \Delta\phi^n$ before adjustment for tangency boundary condition.

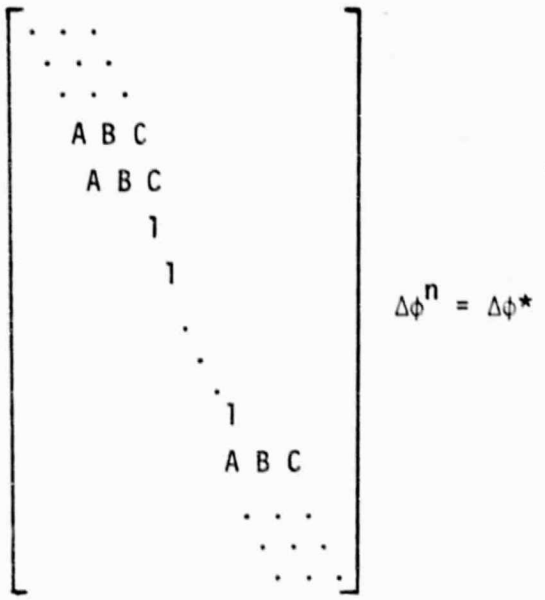

(b) Tridiagonal adjustment if and only if $k = k_{lower}$ or k_{lower}

Fig. 3. Adjustment of ξ-tridiagonal along $k = k_{lower}$ or $k = k_{upper}$.

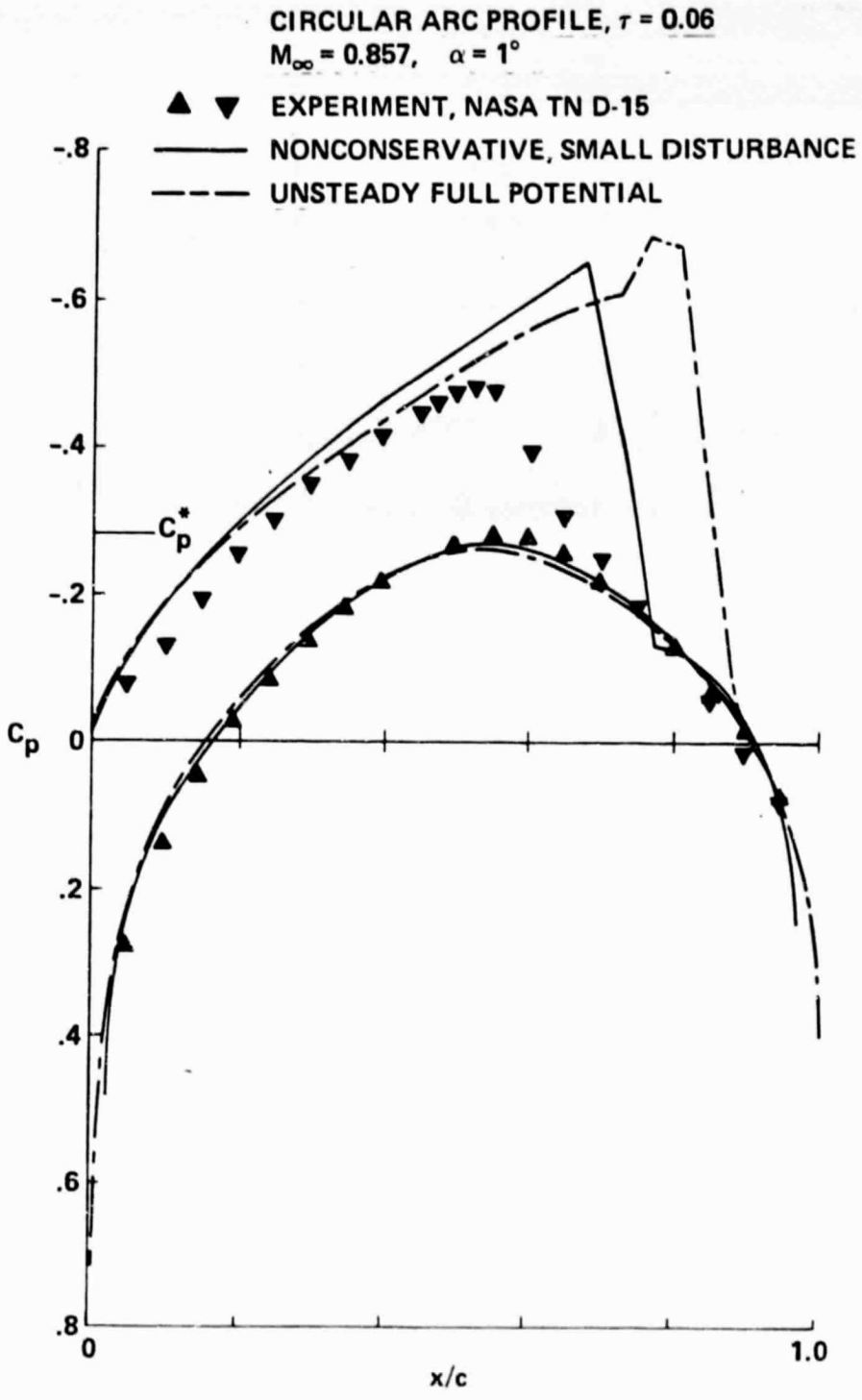

Fig. 4. Steady state flow about biconvex airfoil

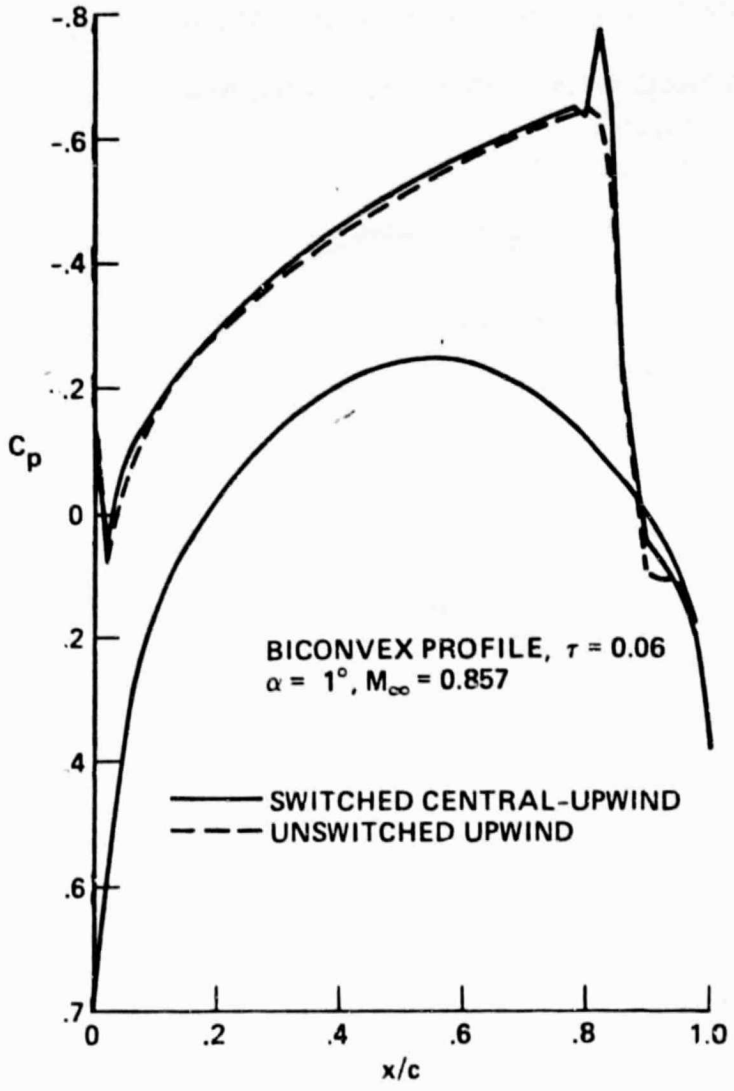

Fig. 5. Comparison of solutions obtained with θ = 1.8 in Eq. 36a.

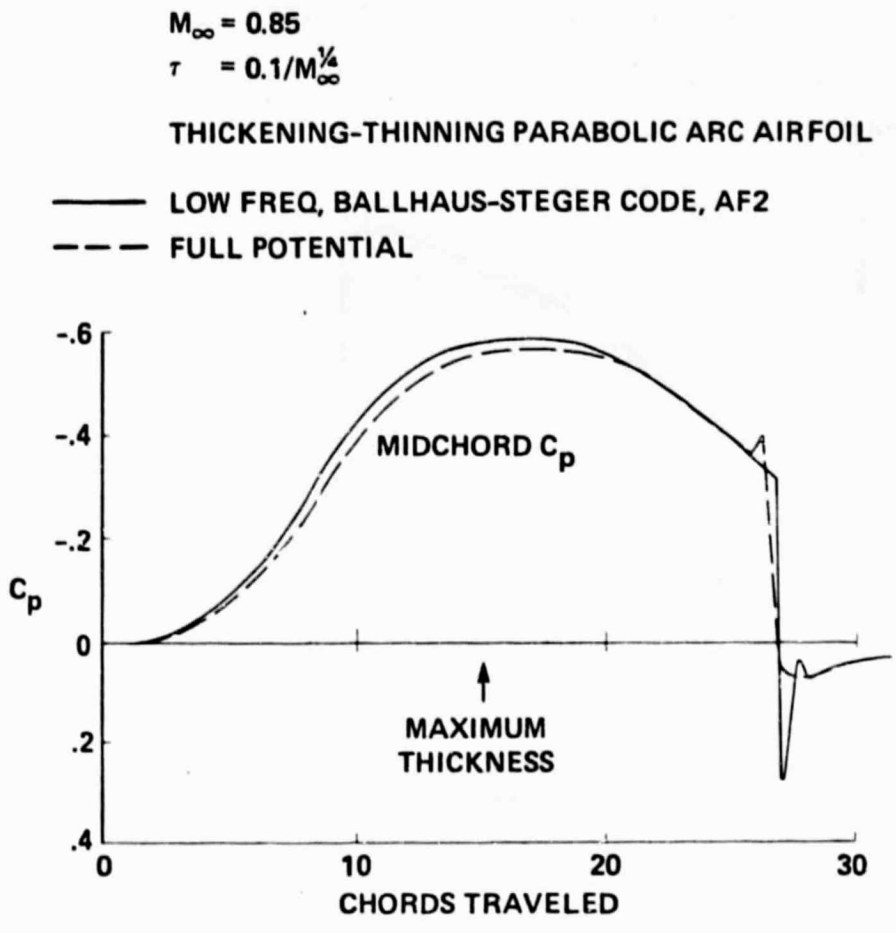

Fig. 6. Mid-chord value of C_p as airfoil thickens then thins

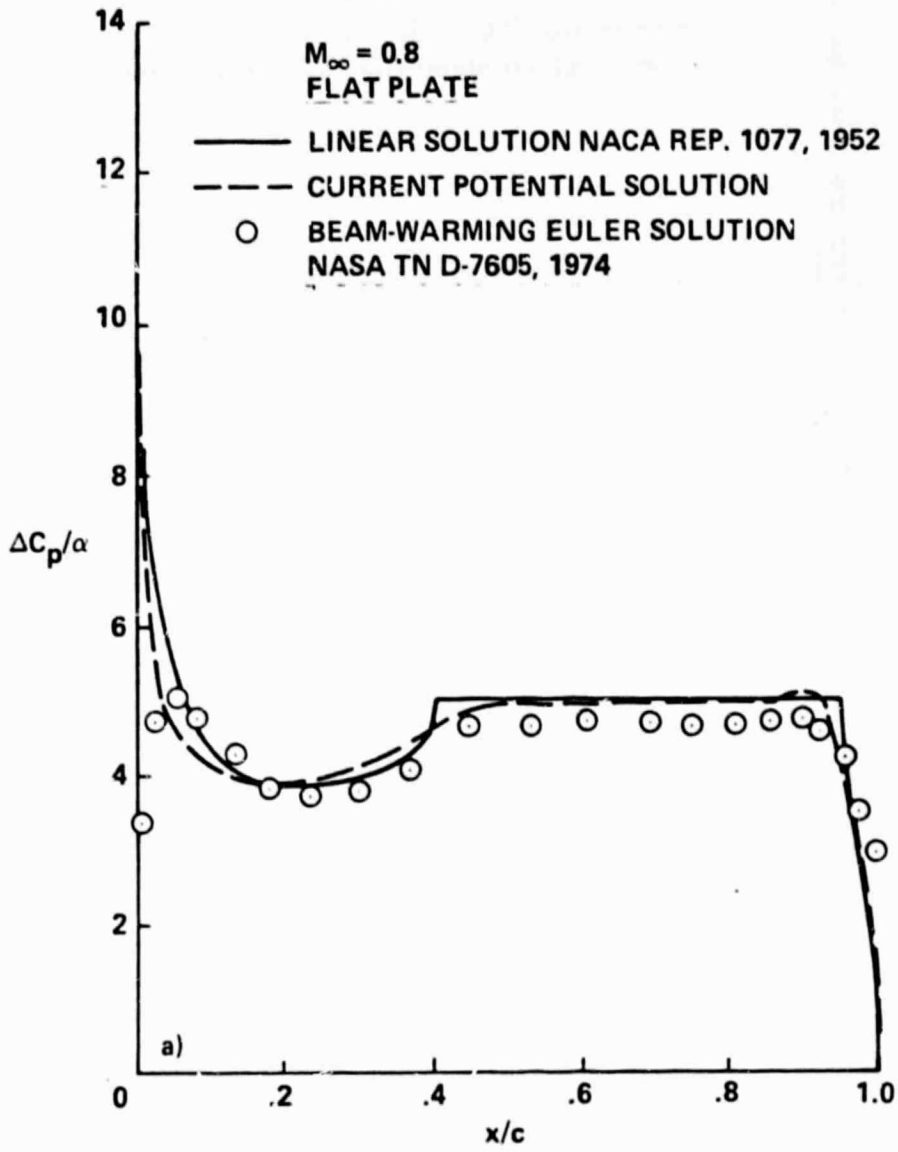

(a) Solution at 0.2 chords of travel from impulsive plunge = 1° of α

Fig. 7. Load distributions along plate for various nondimensional times

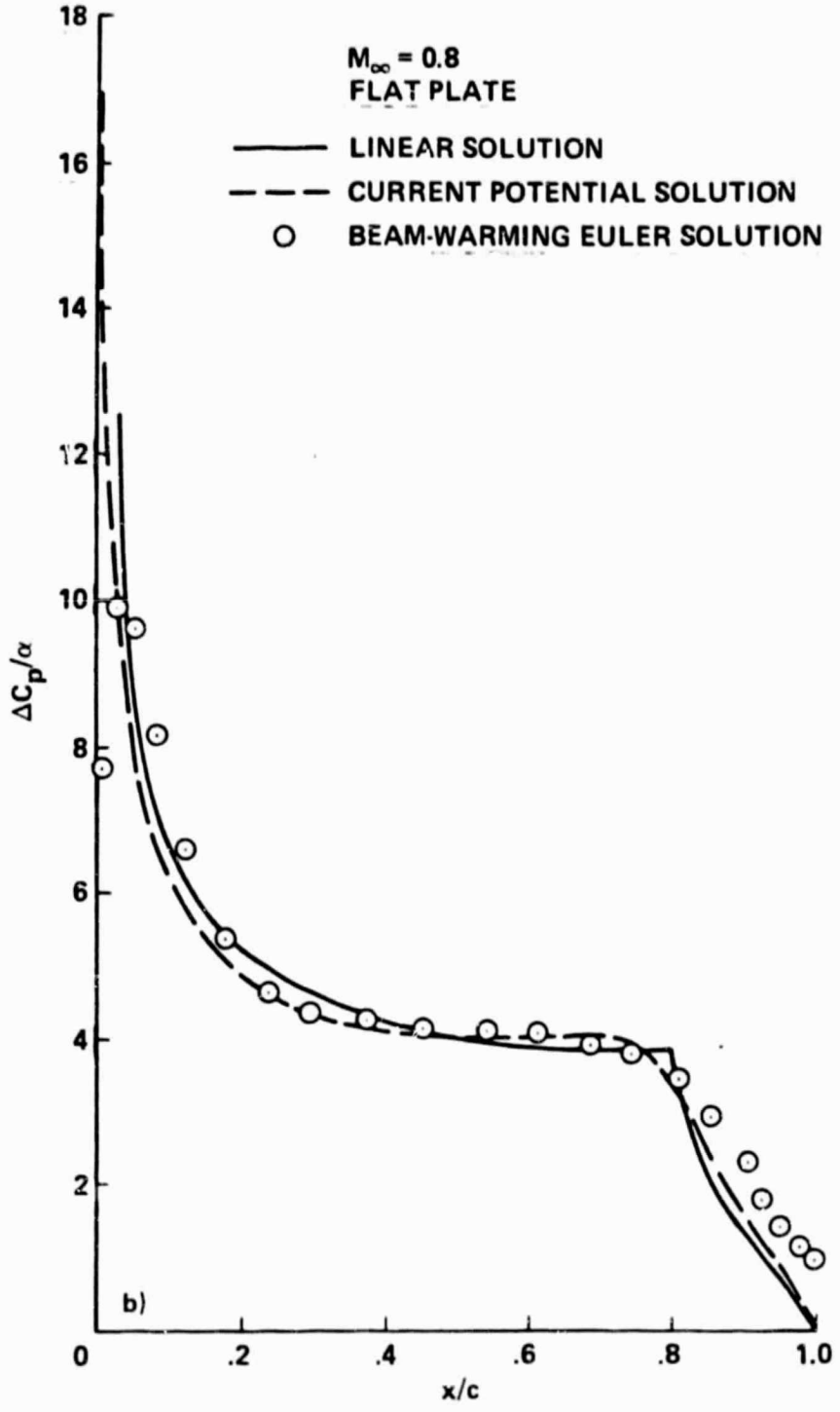

(b) Solution at 0.8 chords of travel

Fig. 7. Continued

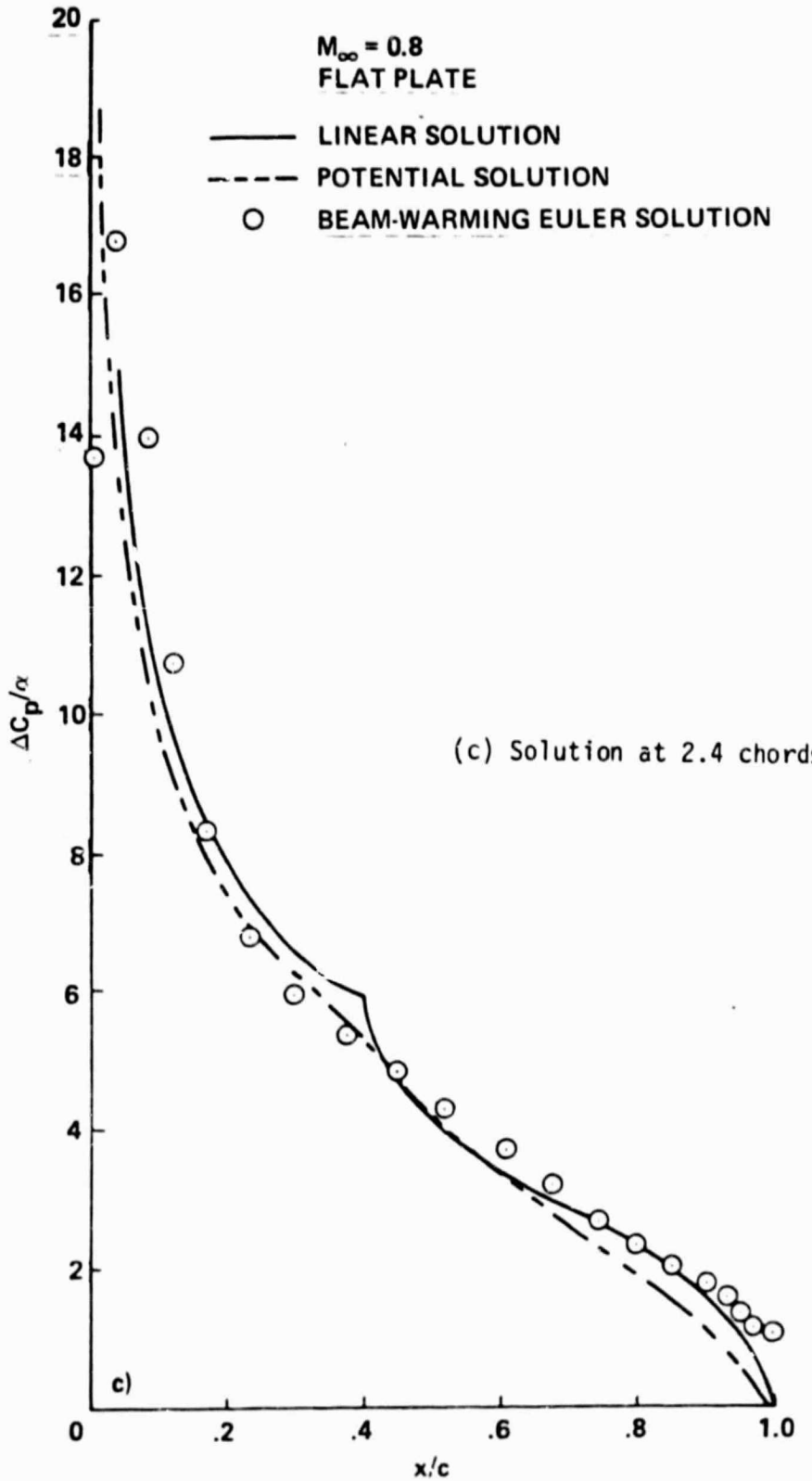

(c) Solution at 2.4 chords of travel

Fig. 7. Continued